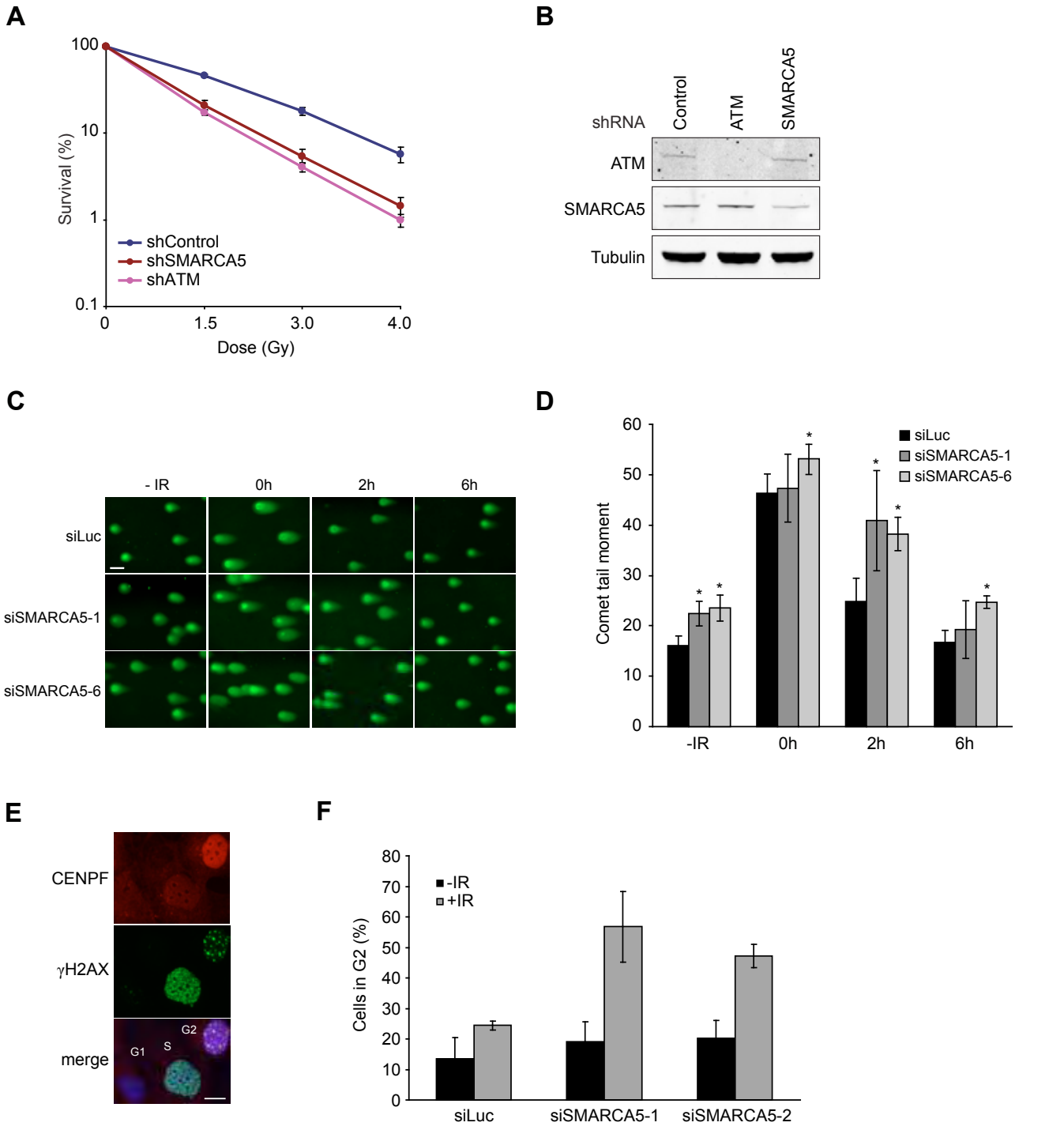

Fig. S1. SMARCA5 depletion renders cells hypersensitive to IR and impairs DSB repair and cell cycle progression after IR. (**A**) VH10-hTERT cells stably expressing an shRNA against SMARCA5 (5′-GATCCCCGTGTTTGCTTCAAAGGAAATTCAAGAGATTTCCTTTGAAGCAAACACTTTTT-3′) or ATM displayed increased IR sensitivity when compared to control cells stably expressing mouse HIF1 shRNA in clonogenic survival assays (van Haaften et al., 2006). Graphs represent the mean ± s.e.m. of 3 independent experiments. (**B**) SMARCA5 and ATM levels were monitored by western blot analysis using WCE of cells in A. Tubulin is a loading control. (**C**) VH10-hTERT cells were transfected with the indicated siRNAs for 72 h, exposed to 20 Gy IR and subjected to neutral comet analysis at the indicated time points using the Comet Assay system (Trevigen) according to the manufacturer's instructions. Representative images are shown. Scale bar, 30 μm. (**D**) Quantification of tail moments using cells from C. Comet tail moments were scored using Comet Score software (TriTek). Tail moments for each condition were calculated for at least 100 cells per data point. The mean ± s.e.m. of 3 experiments is shown. Statistical significance was established at each timepoint using a student t-test. **P*<0.05, compared with siLuc (control). (**E**) Knockdown of SMARCA5 induces a G2 cell cycle arrest after exposure of cells to IR. U2OS cells were exposed to 5 Gy IR or left untreated and after 18 h immunostained for γH2AX and CENP-F (using anti-CENP-F antibody; Santa Cruz). DNA was stained with DAPI. The levels of CENP-F staining distinguished G1, S and G2 cells. Scale bar, 10 μm. (**F**) The percentage of G2 cells ± s.e.m. is presented. More than 120 nuclei were scored per sample in at least 2 independent experiments.

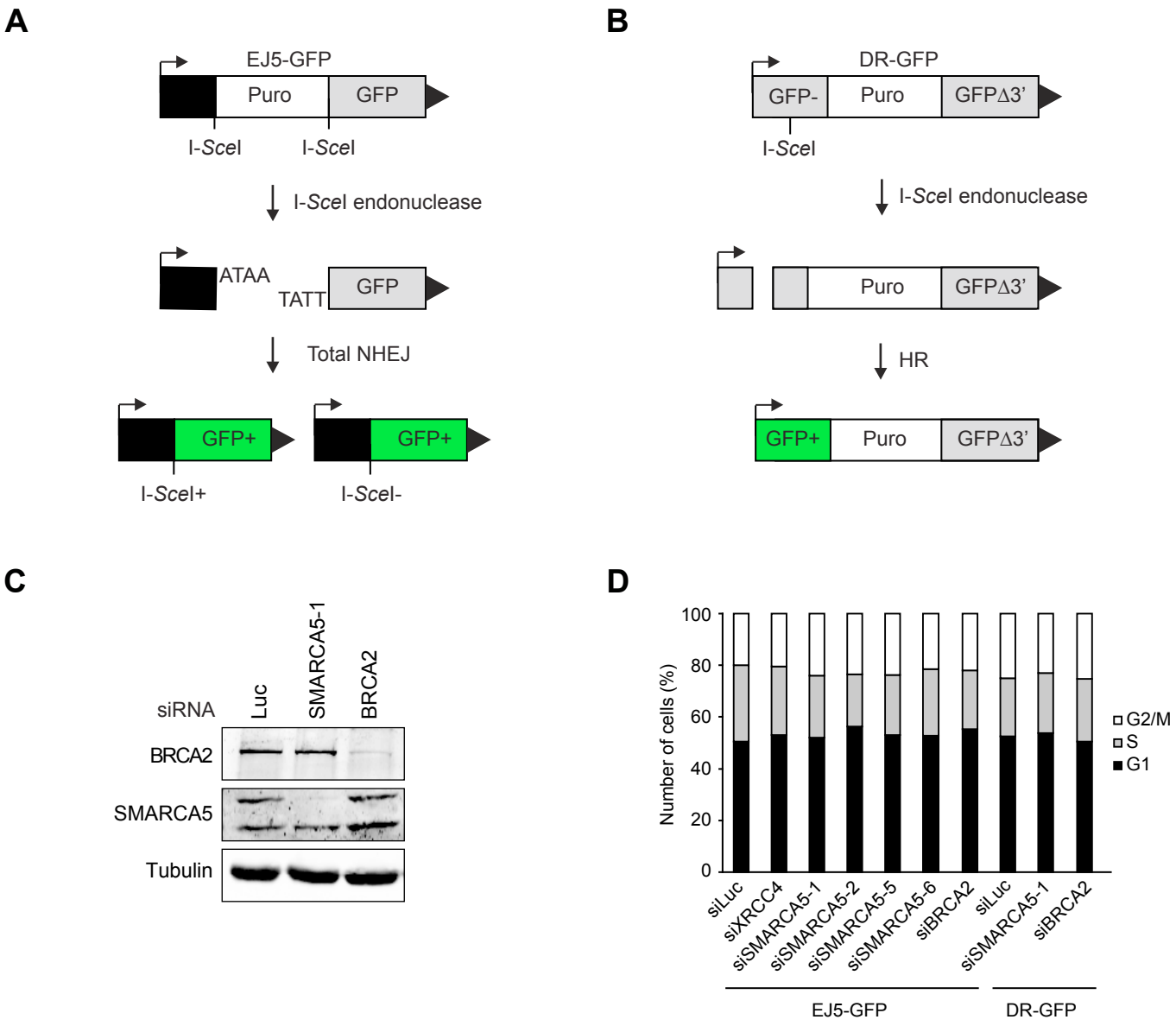

Fig. S2. SMARCA5 depletion does not affect cell cycle progression in NHEJ and HR reporter cell systems. (**A**) Schematic representation of a reporter system for NHEJ. EJ5-GFP consists of a promoter that is separated from a GFP cassette by insertion of a puromycin resistance marker flanked by I-S*ce*I recognition sites (Bennardo et al., 2008). After transient expression of I-S*ce*I and subsequent cleavage at these sites, NHEJ (either error-free or error-prone) will fuse the promoter to GFP and restore expression. (**B**) Schematic representation of a reporter system for HR. DR-GFP consists of two GFP alleles that are non-functional due to the insertion of an I-S*ce*I recognition site and a 3′ truncation, respectively (Weinstock et al., 2006). After transient expression of I-S*ce*I and subsequent cleavage at the I-S*ce*I recognition site, HR will use the GFPΔ3′ as a template to repair the DSB, which will restore GFP expression. (**C**) SMARCA5 and BRCA2 levels were monitored by western blot analysis using WCE from cells in figure 1D. Tubulin is a loading control. (**D**) HEK293T cells containing the EJ5-GFP or DR-GFP reporter system were transfected with the indicated siRNAs. After 48 h cells were stained with propidium iodide and subjected to FACS. Percentage of cells in G1 (black bar), S (grey bar) and G2/M (white bar) phase is represented. Data shown are the average of 2 independent experiments.

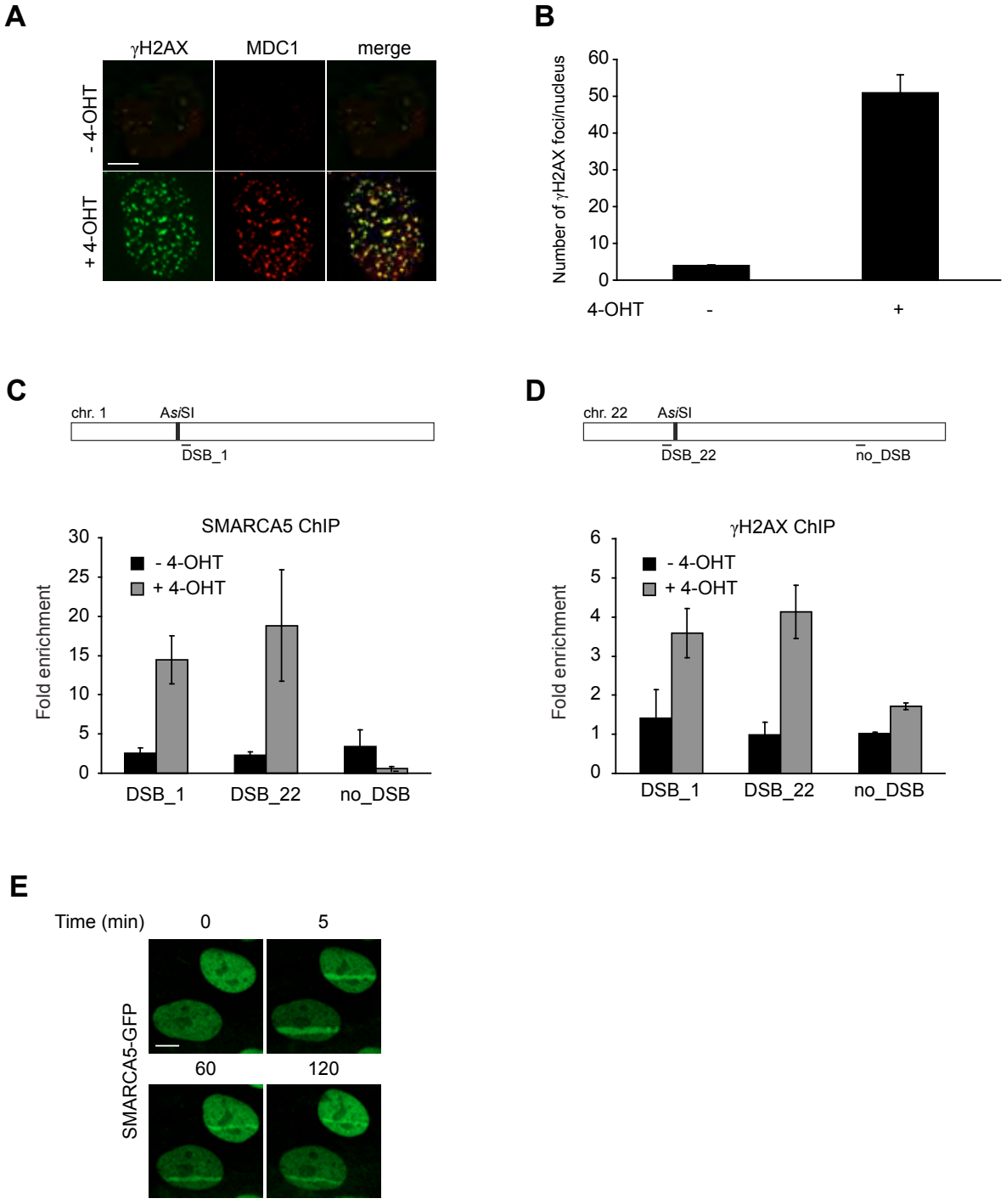

Fig. S3. SMARCA5 accumulates at site-specific DSBs and laser-induced DNA damage. (**A**) U2OS cells containing AsiSI-ER display increased 4-OHT-induced γH2AX and MDC1 foci. Cells containing A*si*SI-ER were untreated or treated with 300 nM 4-OHT for 4 h and subsequently immunostained for γH2AX and MDC1. (**B**) Quantitative analysis of γH2AX focus formation. The average number of foci/nucleus ± s.e.m. is presented. More than 150 nuclei from cells in A were scored per time point in at least 2 independent experiments. (**C**) Site-specific DSBs were induced by treatment of U2OS cells containing A*si*SI-ER with 300 nM 4-hydroxytamoxifen (4-OHT) for 4 hours. Cells were analyzed by ChIP using antibodies against SMARCA5, followed by qPCR using primers at the indicated distances from A*si*SI consensus sequences on chromosome 1 (position 89.231.183) and chromosome 22 (position 19.180.307) as described previously (Iacovoni et al., 2010). The following qPCR primers were used: DSB_1 forward 5′-GATTGGCTATGGGTGTGGAC-3′ and reverse 5′-CATCCTTGCAAACCAGTCCT-3′; DSB_22 forward 5′-CCTTCTTTCCCAGTGGTTCA-3′ and reverse 5′-GTGGTCTGACCCAGAGTGGT-3′; no_DSB forward 5′-CCCATCTCAACCTCCACACT-3′ and reverse 5′-CTTGTCCAGATTCGCTGTGA-3′; GAPDH forward 5′-GAAGGTGAAGGTCGGCGTCA-3′ and 5′-GAAGATGGTGATGGGATTTC-3′. Values for the cleaved (DSB_1 and DSB_22) and non-cleaved (no_DSB; 2 Mb distal to DSB_22) sites were normalized to those for the GAPDH control in ChIP and input samples. ChIP ratios were normalized to input ratios. (**D**) As in C, except that an antibody against γH2AX was used. (**E**) U2OS cells expressing SMARCA5-GFP were laser-irradiated and protein assembly at the damaged area was monitored at the indicated timepoints. Scale bars, 10 μm.

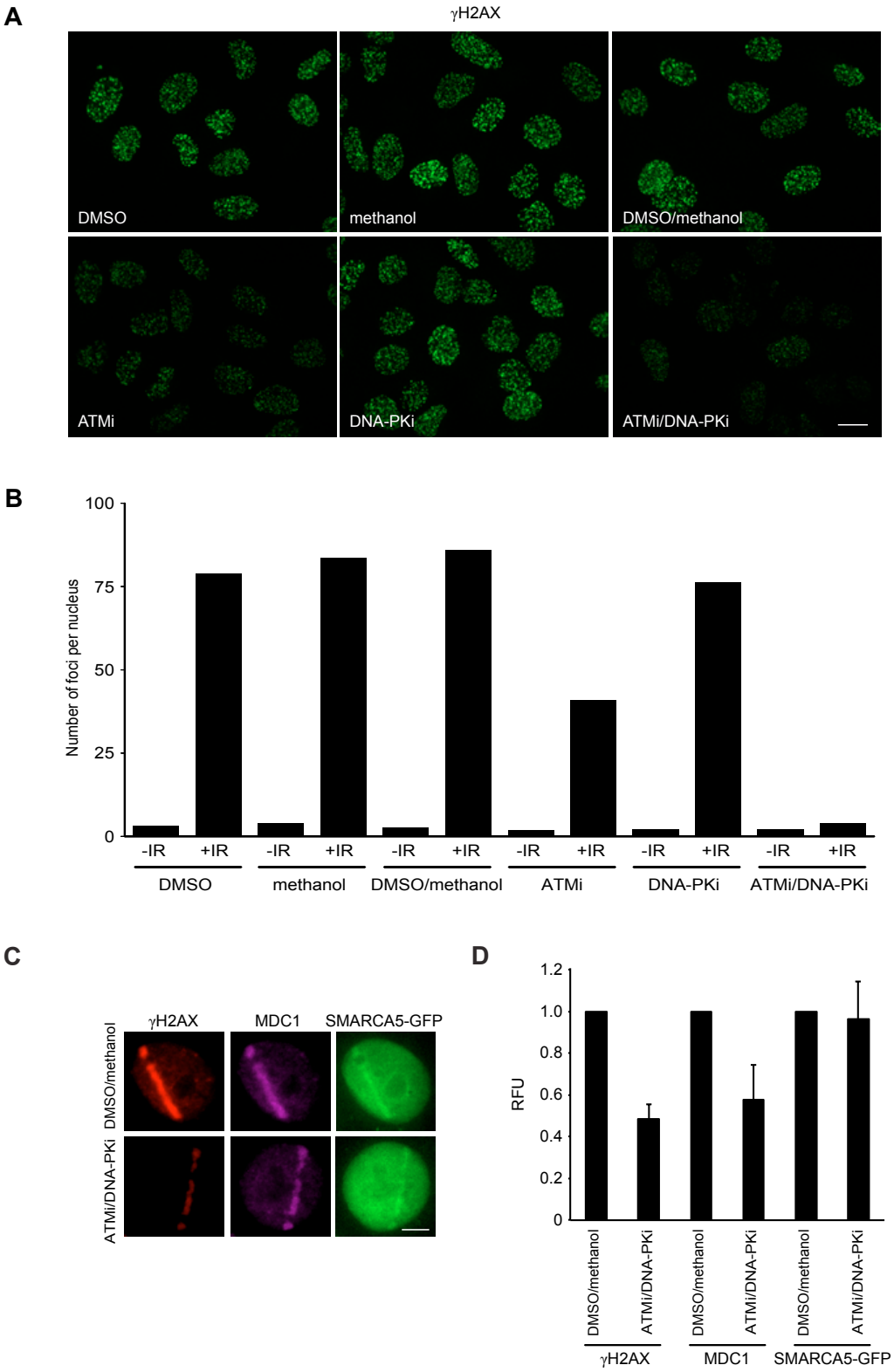

Fig. S4. Effect of ATM/DNA-PK inhibition on γH2AX, MDC1 and SMARCA5 accumulation at sites of DNA damage. (**A**) ATM and DNA-PK inhibition abrogates γH2AX IRIF formation. U2OS cells were treated with DMSO (control for ATM inhibitor), methanol (control for DNA-PK inhibitor) or inhibitors of ATM and DNA-PK, exposed to 2 Gy IR and 30 minutes later immunostained for γH2AX. (**B**) Quantitative representation of γH2AX IRIF formation in C. The average number of γH2AX foci/nucleus is presented. More than 150 nuclei were scored per sample. (**C**) ATM and DNA-PK inhibition reduces γH2AX and MDC1, but not SMARCA5 accumulation at sites of laser-induced DNA damage. U2OS cells expressing SMARCA5-GFP were treated with DMSO (control for ATM inhibitor) and methanol (control for DNA-PK inhibitor), or inhibitors of ATM and DNA-PK, then laser-irradiated and after 15 minutes immunostained for γH2AX and MDC1. (**D**) Quantitative representation of protein assembly at the damaged area in cells from A. Relative Fluorescence Units (RFU) are plotted on a time scale. Graphs represent the mean ± s.e.m. of at least 10 individual cells from 2 independent experiments. The RFU for control cells was set to 1. Scale bars, 10 μm.

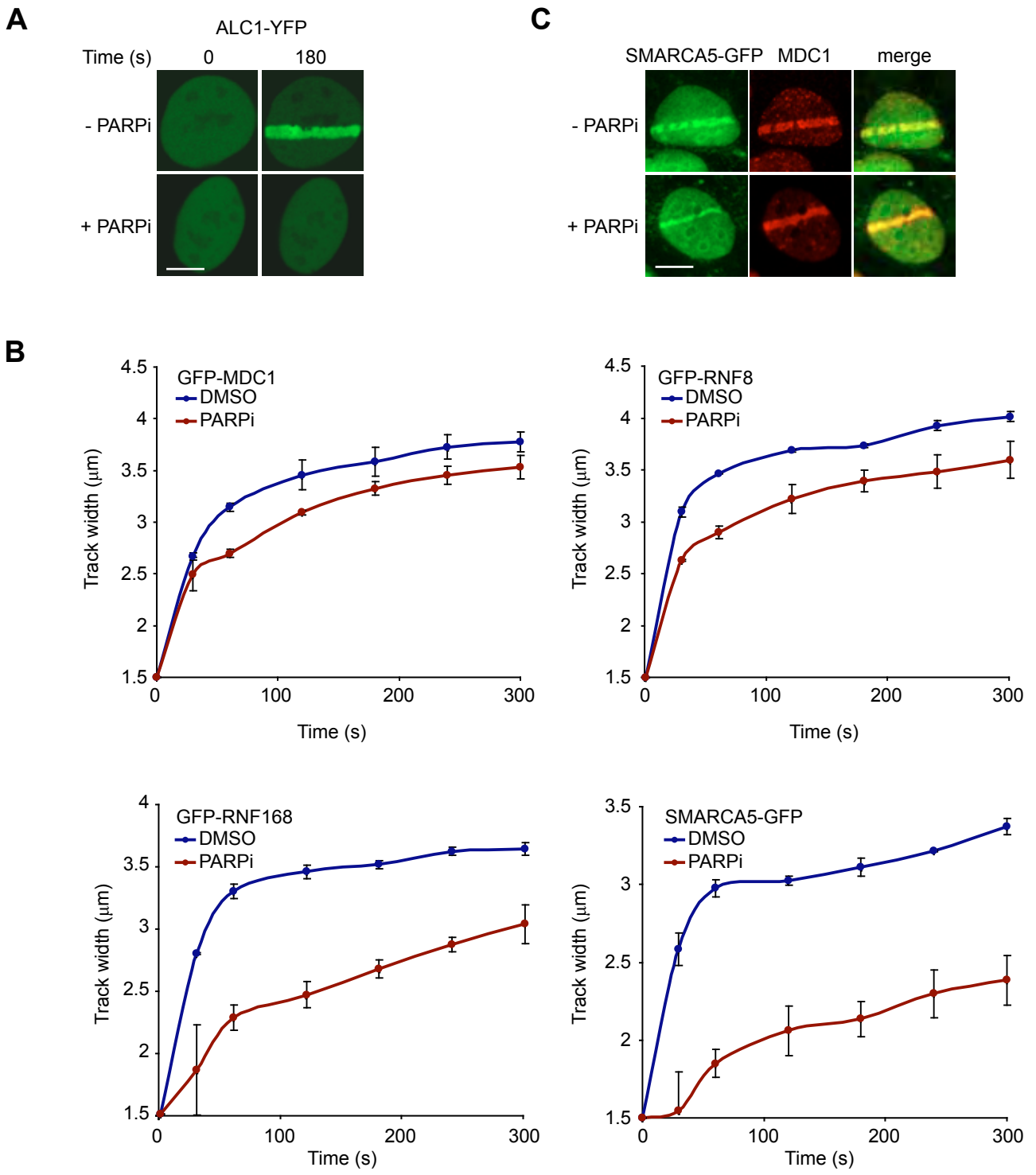

Fig. S5. PARP affects the occupancy of SMARCA5 and factors of the RNF168 cascade throughout damaged chromatin. (**A**) U2OS cells expressing ALC1-YFP were treated with PARP inhibitor or left untreated, and subjected to multi-photon laser-irradiation. Representative images illustrating the effect of PARP inhibition on the accumulation of ALC1-YFP at the indicated timepoints are shown Scale bars, 10 μm. (**B**) As in A, except that U2OS cells expressing GFP-MDC1, GFP-RNF8, GFP-RNF168 or SMARCA5-GFP were used. Moreover, tracks with a width of 1.5 μm were induced using a multiphoton laser and the subsequent increase in track width was measured up to 300 seconds after irradiation. The average track width +/- s.e.m. for at least 20 tracks from two independent experiments is presented. (**C**) As in A, except that U2OS cells expressing SMARCA5-GFP were used to examine the expansion of SMARCA5-GFP and immunostained endogenous MDC1 at 180 seconds after irradiation.

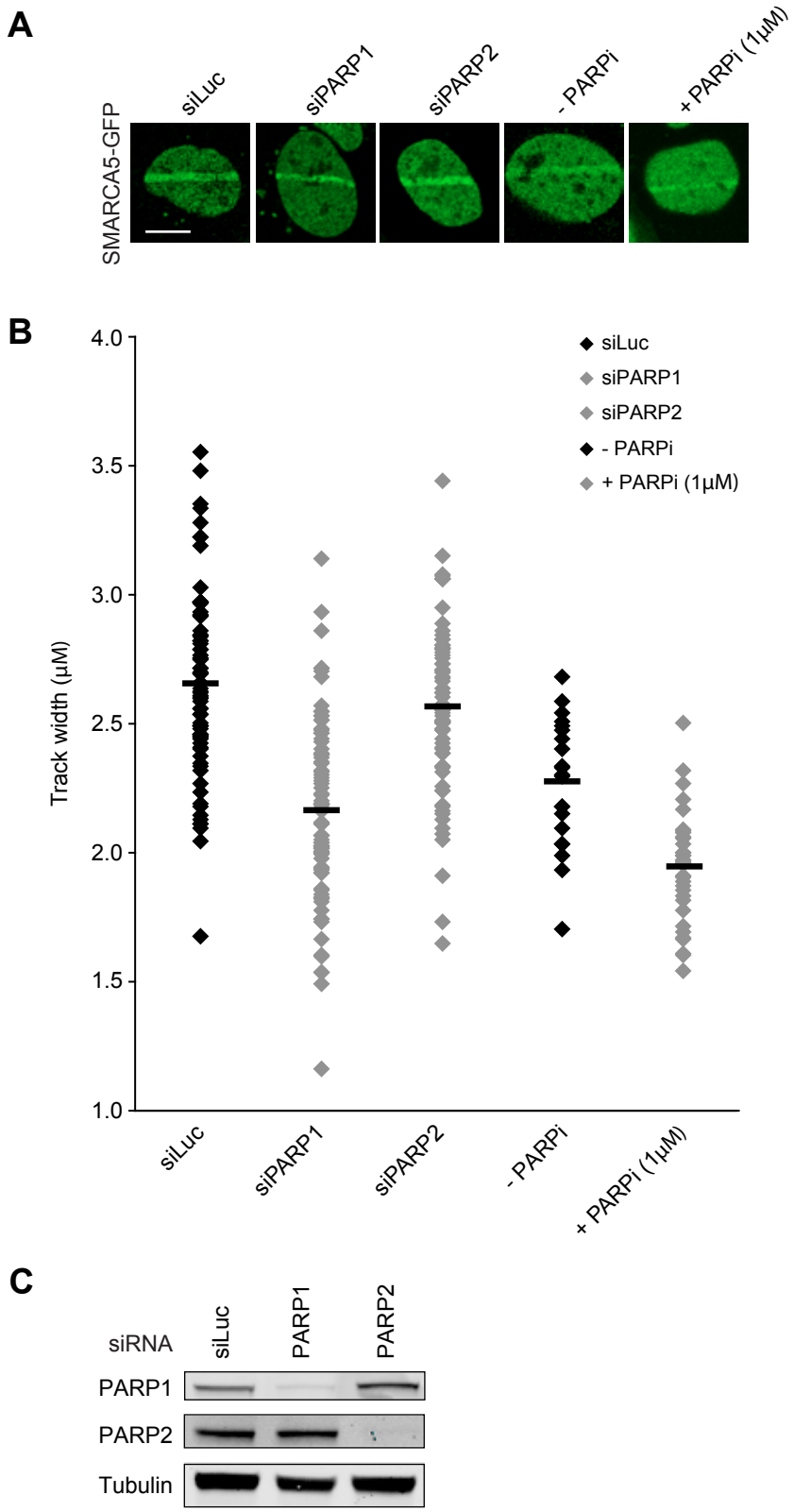

Fig. S6. PARP1, but not PARP2, distributes SMARCA5 throughout damaged chromatin. (**A**) Cells stably expressing SMARCA5-GFP were left untreated, transfected with siRNAs against PARP1 or PARP2, or treated with PARP inhibitor (1μM), then subjected to multi-photon laser-irradiation and analyzed for the expansion of SMARCA5-GFP throughout the damaged compartment. Representative images illustrating the effect of PARP1 knockdown, PARP2 knockdown and PARP1 inhibition (treatment of cells with 1 μM PARP inhibitor kills PARP1, but not PARP2 activity) on the expansion of SMARCA5 are shown. Scale bar, 10 μm. (**B**) Quantitative analysis of the width of DSB-containing laser tracks from cells in A. Laser tracks with a width of 1.5 μm were generated. After 180 s the width of the region showing accumulation of SMARCA5-GFP was measured to determine the increase in track width. Individual measurements ($n \geq 16$) and mean values are presented in a track-width distribution plot. (**C**) PARP1 and PARP2 levels were monitored by western blot analysis using whole cell extracts (WCE) of cells in A. Tubulin is a loading control.

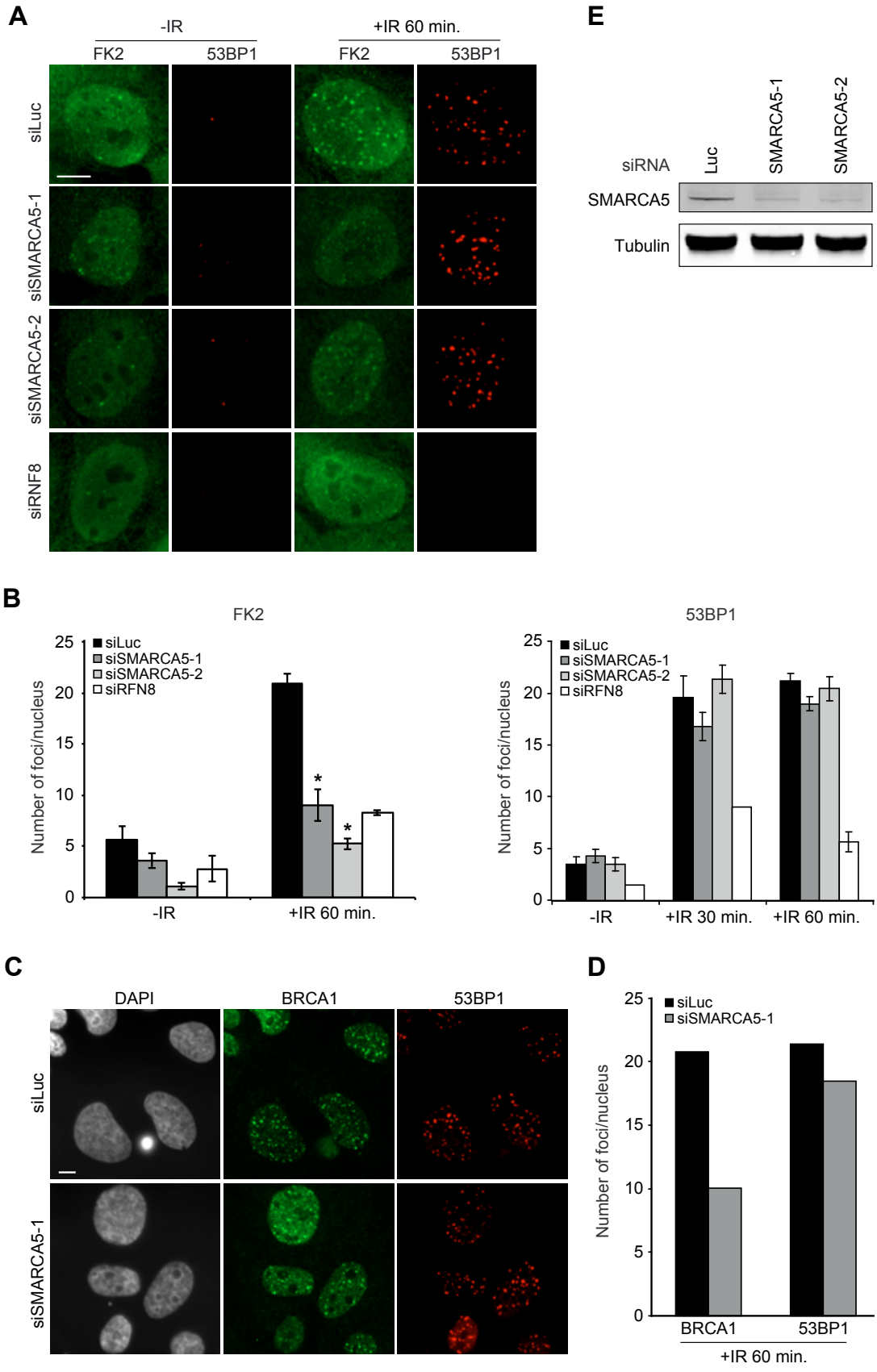

Fig. S7. SMARCA5 depletion does not affect53BP1 IRIF formation. (**A**) Cells were transfected with the indicated siRNAs, exposed to 1 Gy IR and 1 h later immunostained for conjugated ubiquitin (FK2) and 53BP1 to visualize IRIF. Scale bar, 10 μm. (**B**) Quantitative representation of FK2 and 53BP1 IRIF formation in A. The average number of foci/nucleus ± s.e.m. is presented. More than 150 nuclei were scored per time point in independent experiments. **P*<0.05, compared with siLuc (control). (**C**) As in A, except that cells were immunostained for BRCA1 and 53BP1. Scale bar, 10 μm. (**D**) As in B, except for cells from C. (**E**) SMARCA5 levels were monitored by western blot analysis using WCE of cells in A–D. Tubulin is a loading control.

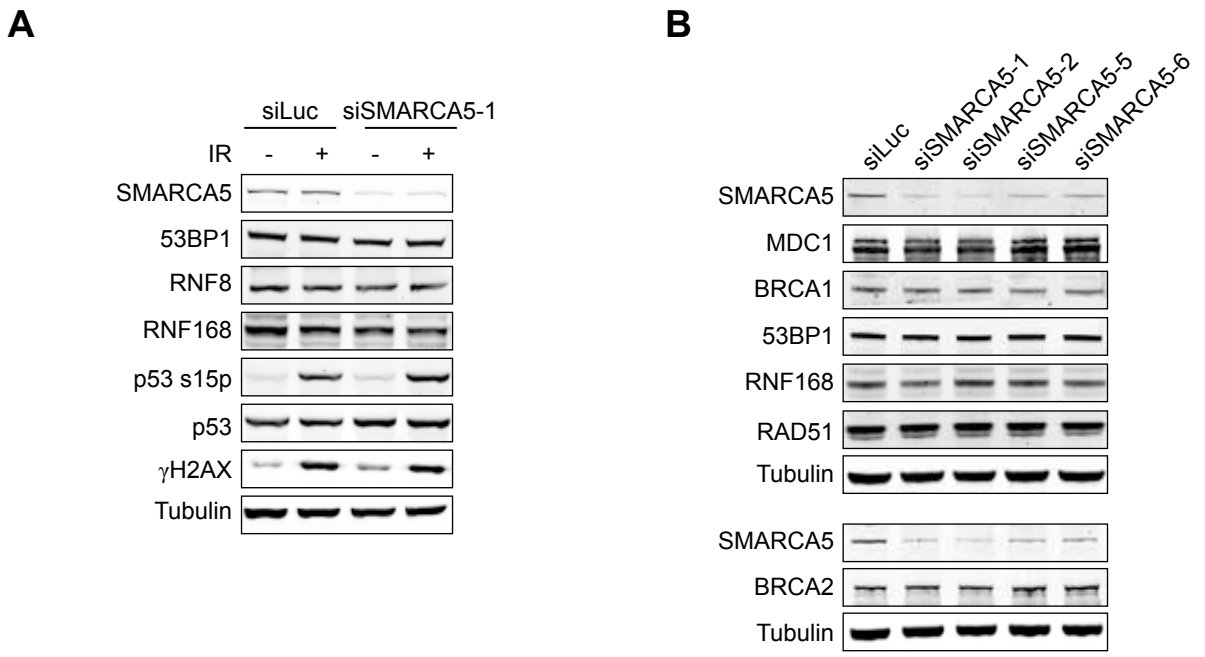

Fig. S8. SMARCA5 depletion does not affect the expression levels of DDR proteins. (**A**) SMARCA5 knockdown does not affect the expression levels of several DDR proteins. U2OS cells were transfected with the indicated siRNAs and left untreated or irradiated with 10 Gy IR. 1 h later WCE were prepared and protein levels were monitored by western blot analysis. Anti-53BP1 (Novus Biologicals), anti-p53 (Santa Cruz), anti-p53 S15p (Cell Signaling), anti-RNF8 (Abcam) and anti-BRCA2 (AB-1, Oncogene) antibodies were used. (**B**) As in A, except that cells were not irradiated.

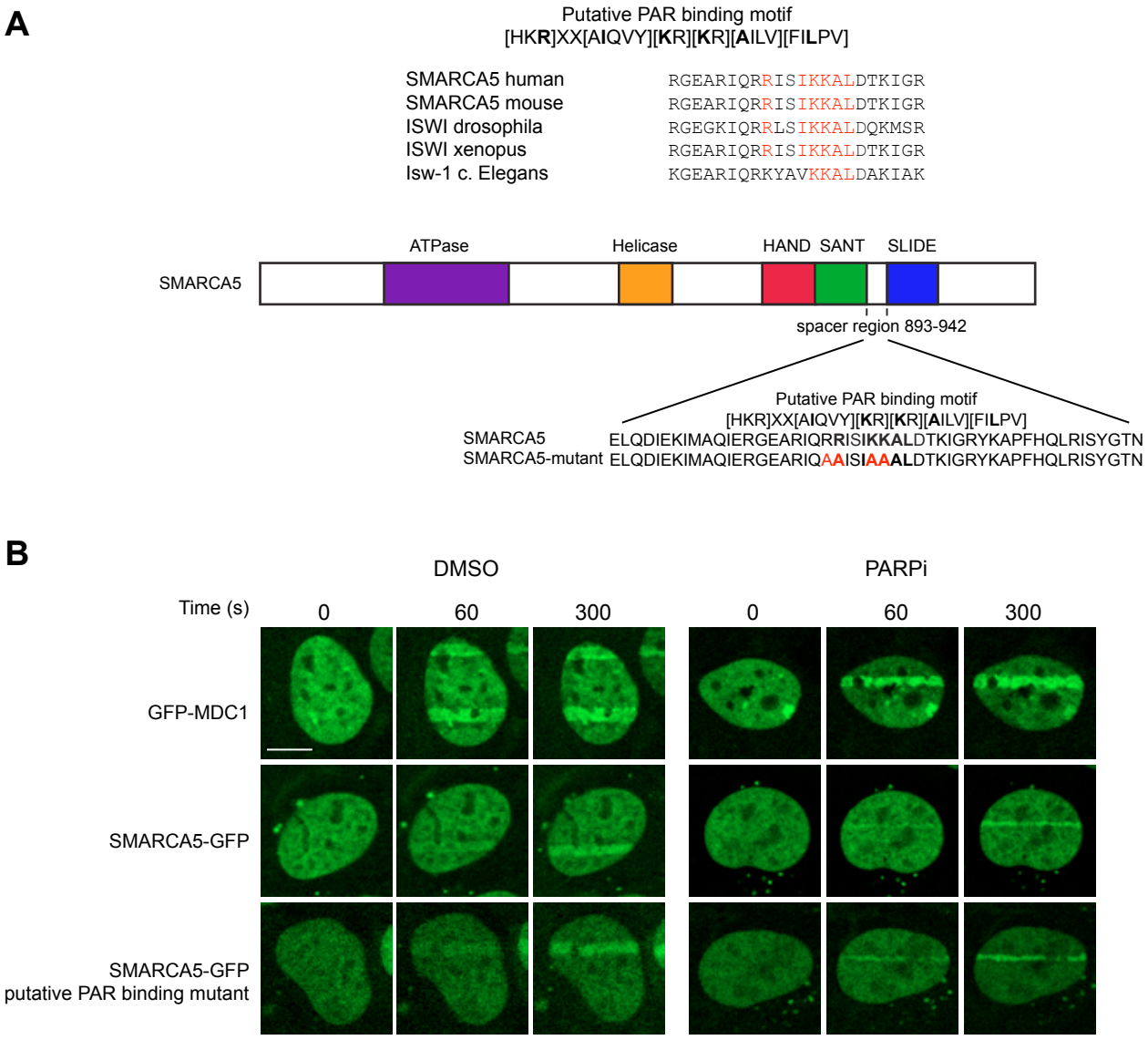

Fig. S9. The putative PAR binding domain of SMARCA5 is not required for its accumulation and spreading in damaged chromatin. (**A**) Schematic representation of the different functional domains in the SMARCA5 protein. A highly conserved putative PAR binding motif was found in the spacer region (893-943) located between the SANT and SLIDE domains. A SMARCA5 mutant was generated in which four conserved residues (two arginine residues and two lysine residues) in the putative PAR binding motif were substituted for alanine residues (indicated in red). (**B**) U2OS cells expressing GFP-MDC1, SMARCA5-GFP or the SMARCA5-GFP putative PAR binding mutant were treated with PARP inhibitor or left untreated and then subjected to multi-photon laser-irradiation. Scale bar, 10 μm.